05 Apr 1995, 1:30 pm - 3:30 pm

Efficient Evaluation of Dynamic Impedance

Gao Lin
Dalian University of Technology, Dalian, China

Huai-hai Chen
Nanjing University of Aeronautics and Astronautics, Nanjing, China

Proceedings: Third International Conference on Recent Advances in Geotechnical Earthquake Engineering and Soil Dynamics
April 2-7, 1995; Volume III, St. Louis, Missouri

Efficient Evaluation of Dynamic Impedance

Paper No. 5.07

Gao Lin
Dalian University of Technology
Dalian, China

Huai-hai Chen
Nanjing University of Aeronautics and Astronautics
Nanjing, China

SYNOPSIS An efficient algorithm for the calculation of dynamic impedance of viscoelastic multi-layered media is presented. The wavenumber integral over infinite limits are split into two sub-intervals, the first one is dominated by the plane waves while the secend is dominated by the surface Rayleigh waves. Though the integrand of the first one is characterized by dense oscillations and sharp peaks, its integration covers very narrow range and can be evaluated sufficiently accurately with dense sampling points. The integrand of second one varies very smoothly and can be dertermined analytically, the integration is easy to perform. The advantages of the present approach is that high degree of accuracy could be achieved, while the computational effort is reduced to a great extent.

INTRODUCTION

The dynamic impedance of infinite halfspace plays an important role in the study of soil-structure interaction effects. For the solution of such wave problems in layered elastic media, the transfer matrices method proposed by Thomson and Haskell has found widespread use in earthquake engineering. However, two major numerical difficulties are inherently associated with its application to practical engineering problems. First, the calculation of exponential terms often leads to overflow of the computer figures or loss of significant figures as the number of layers increases. Second, a great deal of computational effort is devoted to the evaluation of wavenumber integral over infinite limits. The kernels of the integral are complex functions with rapidly oscillatory behavior and the functions are obtained through complicated matrix operations, their evaluation requires much CPU time. A number of methods have been proposed to overcome these difficulties. Dukin (1965) and Knopoff(1965) suggested alternate matrix formulation to avoid loss of significant figures. Xu and Mal(1984) represented the kernel function by means of a series of Chebyshev polynomials in the domain with irregularly oscillatory properties and used an adaptive integration scheme to minimize computational efforts. These approaches improved the situation to a certain extent. In this paper, a new procedure based on the analysis of physical properties of wave equations is presented, the overflow of exponentials is thoroughly avoided, high degree of accuracy could be achieved, in addition, the computational effort is reduced to a great extent. The treatment may be extended to three-dimensional problem, although for illustrative purposes only two-dimensional surface problems are specifically tackled.

FORMULATION OF THE BASIC EQUATIONS

The horizontally layered elastic half-space and its coordinate system is shown in Fig.1. The mth layer is bounded above by the plane $x_2=-h_{m-1}$ and below by the plane $x_2=-h_m$, its thickness is d_m, its modules of elasticity, shear modules of elasticity and Poission's ratio are E_m, G_m, and ν_m respectively. It has P and S wave speeds C_{pm} and C_{sm} respectively.

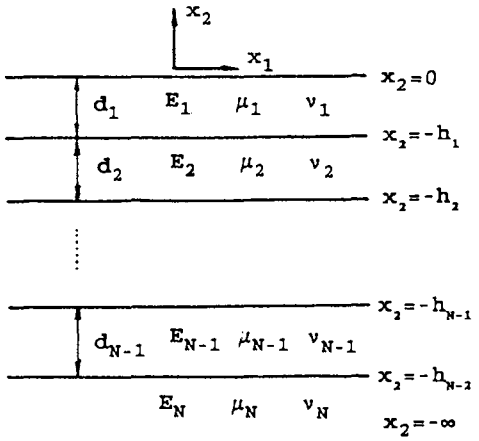

Fig.1 Schematic Representation of Layered Halfspace

In case of viscoelastic medium, the corresponding constants are expressed in the following form

$$\begin{aligned} E_m^* &= E_m(1+2i\zeta_p) \\ G_m^* &= G_m(1+2i\zeta_s) \\ C_{pm}^* &= C_{pm}\sqrt{(1+2i\zeta_p)} \\ C_{sm}^* &= C_{sm}\sqrt{(1+2i\zeta_s)} \end{aligned} \qquad (1)$$

where ζ_p and ζ_s are coefficients characterizing energy loss in hysterectic media. For abbreviation the symbols are omitted hereinafter.

Let u_1 and u_2 denote the displacement components

and σ_{11} σ_{22} and σ_{12} denote the stress components for the mth layer. For a homogeneous, isotropic medium, it is convenient to introduce potentials ϕ and ψ such that

$$\begin{Bmatrix} u_1 \\ u_2 \end{Bmatrix} = \begin{bmatrix} \frac{\partial}{\partial X_1} & -\frac{\partial}{\partial X_2} \\ \frac{\partial}{\partial X_2} & \frac{\partial}{\partial X_1} \end{bmatrix} \begin{Bmatrix} \phi \\ \psi \end{Bmatrix} \tag{2}$$

$$\begin{Bmatrix} \sigma_{11} \\ \sigma_{22} \\ \sigma_{12} \end{Bmatrix} = \begin{bmatrix} \lambda\nabla^2+2\mu\frac{\partial^2}{\partial X_1^2} & -2\mu\frac{\partial^2}{\partial X_1 \partial X_2} \\ \lambda\nabla^2+2\mu\frac{\partial^2}{\partial X_2^2} & -2\mu\frac{\partial^2}{\partial X_1 \partial X_2} \\ 2\mu\frac{\partial^2}{\partial X_1 \partial X_2} & \mu\left(\frac{\partial^2}{\partial X_1^2}-\frac{\partial^2}{\partial X_2^2}\right) \end{bmatrix} \begin{Bmatrix} \phi \\ \psi \end{Bmatrix} \tag{3}$$

where λ and μ are Lame constants of the layer, $\mu=G_m$.

We solve the problem in the frequency domain and suppress time dependence $\exp(-i\omega t)$ in all field quantities, keeping in mind ω is the circular frequency. ϕ and ψ satisfy wave equation within each layer

$$\begin{aligned} \nabla^2\phi+K_p^2\phi=0 \\ \nabla^2\psi+K_s^2\psi=0 \end{aligned} \tag{4}$$

where $$K_p=\omega/C_{pm} \quad , \quad K_s=\omega/C_{sm} \tag{5}$$

Then using Fourier transform defined by

$$\begin{aligned} \bar{f}(\xi, x_2, \omega) &= \int_{-\infty}^{\infty} f(x_1, x_2, \omega)\, e^{-i\xi x_1} dx_1 \\ f(x_1, x_2, \omega) &= \frac{1}{2\pi}\int_{-\infty}^{\infty} \bar{f}(\xi, x_2, \omega)\, e^{i\xi x_1} d\xi \end{aligned} \tag{6}$$

We obtain transformed solution of (4)

$$\begin{aligned} \bar{\phi}(\xi, x_2, \omega) &= A_1(\xi)\exp(k_1 x_2)+A_2(\xi)\exp(-k_1 x_2) \\ \bar{\psi}(\xi, x_2, \omega) &= B_1(\xi)\exp(k_2 x_2)+B_2(\xi)\exp(-k_2 x_2) \end{aligned} \tag{7}$$

where

$$\begin{aligned} k_1 &= \begin{cases} i\sqrt{k_p^2-\xi^2} & R_l(k_p) \geq \xi \\ \sqrt{\xi^2-k_p^2} & R_l(k_p) < \xi \end{cases} \\ k_2 &= \begin{cases} i\sqrt{k_s^2-\xi^2} & R_l(k_s) \geq \xi \\ \sqrt{\xi^2-k_s^2} & R_l(k_s) < \xi \end{cases} \end{aligned} \tag{8}$$

in which coefficients A_1, B_1, A_2, B_2 are functions of the transform variable ξ. Let $\{C\}$ denote the coefficient vector $[A_1, B_1, A_2, B_2]^T$ and $\{S(x_2)\}$ the transformed displacement-stress vector $[u_1, u_2, \sigma_{12}, \sigma_{22}]^T$ in each layer. It can be shown from Eq. (2) (3) and (7), that $\{S(x_2)\}$ in the mth layer may be represented by means of the matrix products.

$$\{S(x_2)\}_m = [T]_m [E]_m \{C\}_m \tag{9}$$

Where

$$[E]_m = Diag.\,[\exp(k_1 x_2), \exp(k_2 x_2), \exp(k_1, x_2), \exp(-k_2 x_2)]_m \tag{10}$$

$$[T]_m = \begin{bmatrix} i\xi & k_2 & i\xi & -k_2 \\ k_1 & -i\xi & -k_1 & -i\xi \\ 2\mu i\xi k_1 & \mu(2\xi^2-k_s^2) & -2\mu i\xi k_1 & \mu(2\xi^2-k_s^2) \\ \mu(2\xi^2-k_s^2) & -2\mu i\xi k_2 & \mu(2\xi^2-k_s^2) & 2\mu i\xi k_2 \end{bmatrix} \tag{11}$$

Then by successively applying the interface continuity conditions, for example at $x_2=h_m$

$$\{S(h_m)\}_m = \{S(h_m)\}_{m+1} \tag{12}$$

we have

$$[T]_m [E(h_m)]_m \{C\}_m = [T]_{m+1} [E(h_m)]_{m+1} \{C\}_{m+1} \tag{13}$$

or

$$\{C\}_m = [E(h_m)]_m^{-1} [T]_m^{-1} [T]_{m+1} [E(h_m)]_{m+1} \{C\}_{m+1} \tag{14}$$

Let

$$[D]_m = [E]_m^{-1} [T]_m^{-1} [T]_{m+1} [E]_{m+1} \tag{15}$$

we can see that

$$\{C\}_m = [D]_m \{C\}_{m+1} \tag{16}$$

The displacement-stress vector at the top surface is related to the coefficients of the bottom half-space

$$\{S\}_0 = [T]_1 [D] \{C\}_N \tag{17}$$

Where

$$[D] = [D]_1 [D]_2 \cdots [D]_{N-1} \tag{18}$$

Furthermore, introduce

$$\begin{aligned} [\theta]_i &= [E(h_i)]_i [E(h_{i+1})]_i^{-1} [T]_i^{-1} [T]_{i+1} \\ [\theta] &= [\theta]_1 [\theta]_2 \cdots [\theta]_{N-1} \end{aligned} \tag{19}$$

we have

$$\{S\}_0 = [T]_1 [\theta]\, [E(h_{N-1})]_N \{C\}_N \tag{20}$$

The radiation condition in the bottom half-space requires that

$$\{C\}_N = [A_1\ B_1\ A_2\ B_2]_N^T = [A_1\ B_1\ 0\ 0]_N^T \tag{21}$$

Let [P] denotes

$$[P] = [T]_1 [\theta]\, [E(h_{N-1})]_N \tag{22}$$

and partition [P] into second order matrices according to

$$[P] = \begin{bmatrix} P_{11} & P_{12} \\ P_{21} & P_{22} \end{bmatrix} \tag{23}$$

From (20) and (21), the displacements and stresses at the top surface are established as

$$\begin{Bmatrix} \overline{u_1}(x_2=0) \\ \overline{u_2}(x_2=0) \end{Bmatrix} = [F] \begin{Bmatrix} \overline{\sigma_{12}}(x_2=0) \\ \overline{\sigma_{22}}(x_2=0) \end{Bmatrix} \tag{24}$$

where

$$[F] = [P_{11}]\,[P_{21}]^{-1} \tag{25}$$

And inverse Fourier transform gives

$$\begin{Bmatrix} u_1(x_1,0,\omega) \\ u_2(x_1,0,\omega) \end{Bmatrix} = \frac{1}{2\pi}\int_{-\infty}^{\infty} \begin{bmatrix} F_{11} & F_{12} \\ F_{21} & F_{22} \end{bmatrix} \begin{Bmatrix} \overline{\sigma_{12}}(\xi,0,\omega) \\ \overline{\sigma_{22}}(\xi,0,\omega) \end{Bmatrix} e^{i\xi x_1} d\xi \tag{26}$$

Once the relations between the surface displacements and stresses having been found, it is not difficult to get the dynamic impedance of the surface foundation.

As an example, the surface compliance of uniformly distributed load over a width of b with their resultant equals unity is studied.

Suppose forces are acting in the x_1 direction, then

$$\overline{\sigma_{12}}(\xi,0,\omega) = \frac{1}{b}\int_{-\frac{b}{2}}^{\frac{b}{2}} e^{-i\xi x_1} dx_1 = \frac{2}{b\xi}\sin\frac{b\xi}{2} \tag{27}$$

we have

$$\begin{Bmatrix} u_{11}(x_1,0,\omega) \\ u_{21}(x_1,0,\omega) \end{Bmatrix} = \frac{1}{2\pi}\int_{-\infty}^{\infty} \begin{bmatrix} F_{11} \\ F_{21} \end{bmatrix} \left(\frac{2}{b\xi}\sin\frac{b\xi}{2}\right) e^{i\xi x_1} d\xi \tag{28}$$

Taking into consideration the symmetrical and antisymmetrical properties of the odd and even components of $\exp(i\xi x_1)$, (28) can be further simplified to

$$\begin{Bmatrix} u_{11} \\ u_{21} \end{Bmatrix}_{x_2=0} = \frac{1}{\pi}\int_0^{\infty} \begin{bmatrix} F_{11}\cos x_1\xi \\ iF_{21}\sin x_1\xi \end{bmatrix} \left(\frac{2}{b\xi}\sin\frac{b\xi}{2}\right) d\xi \tag{29}$$

In the similar manner, if the forces acting in the x_2 direction, we have

$$\begin{Bmatrix} u_{12} \\ u_{22} \end{Bmatrix}_{x_2=0} = \frac{1}{\pi}\int_0^{\infty} \begin{bmatrix} iF_{12}\sin x_1\xi \\ F_{22}\cos x_1\xi \end{bmatrix} \left(\frac{2}{b\xi}\sin\frac{b\xi}{2}\right) d\xi \tag{30}$$

As the kernel function of the integral [F] are evaluated through complicated matrix operations, it is worth to mention the following points which are very useful for the calculation of [F].

1. Multiplying [P] with any nonzero constants, [F] keeps unchanged. In view of this , the very small factors in the denominator during the matrices operations may be omitted.
2. As $[E(h_{N-1})]_N$ is a diagonal matrix, cancellation of which in the calculation of [P] does not have any influences on the final results of [F]. It has the advantages of avoiding loss of significant figures during matrices multiplications.
3. F_{11} and F_{22} are even functions of ξ, while F_{12} are odd functions of ξ and $F_{12}=-F_{21}$.

TECHNIQUES FOR THE EVALUATION OF WAVENUMBER INTEGRALS

Efficient and accurate numerical evaluation of the wavenumber integrals of the form

$$I = \int_0^{\infty} f(\xi, x_2, \omega) e^{i\xi x_1} d\xi \tag{31}$$

is the major task in the numerical calculation of dynamic impedance. Direct performing the integration associates with great difficulties as the kernel functions of the integral $f(\xi, x_2, \omega)$ are determined through complicated matrices products with exponential terms which often leads to overflow of the computer figures, in addition, the functions behave with sharp peaks and dense oscillations, the larger the integral variable ξ becomes, the more rapid it oscillates. So the key points of the problem turn into the treatment of the exponential terms of the potentials ϕ and ψ, $\exp(-k_1x_2)$ and $\exp(-k_2x_1)$ (see Eq.7). We will discuss it in detail as follows.

Express k_1 and k_2 of the mth layer in the following form

$$k_1 = a_m + ib_m \quad , \quad k_2 = c_m + id_m \tag{32}$$

According to the boundary conditions of wave propagation (Fig. 1) , a_m, b_m, c_m, d_m, are real, and we should have $a_m>0$, $c_m>0$. Then Eq.(7) for the mth layer takes the form

$$\begin{aligned} \overline{\Phi}(\xi,x_2,\omega) &= A_{1m}(\xi)\, e^{a_m x_2} e^{ib_m x_2} + A_{2m}(\xi)\, e^{-a_m x_2} e^{-ib_m x_2} \\ \overline{\Psi}(\xi,x_2,\omega) &= B_{1m}(\xi)\, e^{c_m x_2} e^{id_m x_2} + B_{2m}(\xi)\, e^{-c_m x_2} e^{-id_m x_2} \end{aligned} \tag{33}$$

It should be noted that in the coordinate system as shown in Fig.1. x_2 is always negative, so the terms $\exp(a_m x_2)$ and $\exp(c_m x_2)$ represent downgoing waves in the layer, whereas $\exp(-a_m x_2)$ and $\exp(-a_m x_2)$ represent upgoing waves. The terms $\exp(-a_m x_2)$ and $\exp(-c_m x_2)$ increase in amplitude with x_2 , and at a certain depth, overflow of these exponents takes place. The procedures to overcome these difficulties are suggested as follows.

1. $0<\xi<\mathrm{Re}(K_p)$

As $\mathrm{Re}(K_p)<\mathrm{Re}(K_s)$, we should have $\mathrm{Re}(K_p)>\xi$ and $\mathrm{Re}(K_s)>\xi$. In this case, overflow is caused by the material damping of the medium during wave propagation. Because if no material damping exists, K_p and K_s are real, K_1 and K_2 are pure imaginary (see Eq.8) , it is inevitable that $a_m=0$ and $c_m=0$, no overflow may happen. Only if material damping exist, when $(a_m x_2)$ and $(c_m x_2)$ become large, as a result, overflow of the exponential terms $\exp(-a_m x_2)$ and $\exp(-c_m x_2)$ is induced. However, terms $\exp(-a_m x_2)$ and $\exp(-c_m x_2)$ represent reflected upgoing waves, overflow of $\exp(-a_m x_2)$ and $\exp(-c_m x_2)$ means that downgoing waves $\exp(a_m x_2)$ and $\exp(-c_m x_2)$ loss their significance due to material damping of the medium. This implies that we may assume $A_{2m}(\xi)=0$ and $B_{2m}(\xi)=0$, recognizing that the waves are not propagating further, they are absorbed in this layer. Hence, calculation may be carried out down to the layer, where $(a_m x_2)$ and $(c_m x_2)$ are sufficiently large. It avoids exponential overflow and minimizes ineffective computational effort.

2. $\mathrm{Re}(K_s)<\xi<\infty$

In this case, we have $\xi>\mathrm{Re}(K_s)$ and $\xi>\mathrm{Re}(K_p)$, K_1 and K_2 increase along with the growth of ξ. The amplitudes of a_m and c_m are controlled by the integral variable ξ. Large value of ξ results in

the overflow of the terms $\exp(-a_m x_2)$ and $\exp(-c_m x_2)$. In the similar way, it implies that the downgoing wave loss their significance, so the integration needs not be carried out up to the infinity, but to a certain large value of ξ, beyond which the contribution of the integral reduces to insignificant.

The two cases studied above, i.e. $0<\xi<Re(K_p)$ and $Re(K_s)<\xi<\infty$ correspond to two important phenomena of wave propagation. In the first one, the energy loss of the transmitting waves is caused by the material damping, while in the second one, waves decay due to geometrical factors, or radiating damping, so long as ξ becomes large, wave propagation is restricted in the surface layer, and the wave turns to Rayleigh surface wave.It may also be shown, that the two cases correspond to the conditions where plane waves and Rayleigh waves are dominate, and the range of the first one is much narrower than that of the second one. In other words, among the waves induced by the vibration of the surface foundation, the major part of wave energy is concentrated on the surface waves, besides, the range of S waves is larger than that of the P waves. The distribution of wave energy with respect to the change of Poission's ratio ν among these waves are summarized in the table I (Chen 1993).

Table I. Wave energy distribution (%)

	ν=0.15	ν=0.25	ν=0.45
R wave	71.1	67.4	58.0
S wave	22.2	25.7	40.5
P wave	6.7	6.9	1.5

3. $Re(K_p)\le\xi\le Re(K_s)$

In this case, P waves degenerate into R waves and S waves keeps unchanged. The same treatment as given in the above may be applied.

The main points of the proposed procedure are summarized as follows. For small values of integral variable ξ, plane waves dominate, computations may be carried out down to the layer, where $|a_m x_2|$ or $|c_m x_2|$ become sufficiently large. While for large values of ξ, Rayleigh waves dominate, computations may be restricted only to the surface layers. And keep in mind, that the former range is much narrower than the later one. In view of this , the wave number integral is split into two parts

$$I=\int_0^{\infty} f(\xi,x_2,\omega)\,e^{i\xi x_1}d\xi = \int_0^{\xi_p} f(\xi,x_2,\omega)\,e^{i\xi x_1}d\xi+\int_{\xi_p}^{\xi_u} f(\xi_1,x_2,\omega)\,d\xi \qquad (34)$$

The first term on the right hand side corresponds to the range of plane waves, while the second one corresponds to that of Rayleigh waves, and ξ_u is a upper limit of integration, such that the contribution of R waves becomes insignificant.

For further simplification, (34) is modified as

$$I=I_1+I_2=\int_0^{\xi_a} f(\xi,x_2,\omega)\,e^{i\xi x_1}d\xi+\int_{\xi_a}^{\xi_u} f(\xi,x_2,\omega)\,e^{i\xi x_1}d\xi \qquad (35)$$

where ξ_a is the lower limit of ξ such that wave propagation occurs only in the top layer and the matrix [F] (see Eq.26, 28, 29 and 30) in the integral of I_2 ,can be determined directly as

$$[F]=\frac{1}{\mu(4\xi^2k_1k_2-k_3^2)}\begin{bmatrix} k_2k_s^2 & i\xi(2k_1k_2-k_3) \\ -i\xi(2k_1k_2-k_3) & k_1k_3^2 \end{bmatrix} \qquad (36)$$

where

$$k_3=2\xi^2-k_s^2 \qquad (37)$$

all elastic constants in (36) refer to the top layer. Thus computational effort is reduced to a great extent. It is worth to note, that ξ_a needn't be determined precisely, but may be estimated arbitrarily on the safe side, ξ_u may also be estimated. Or, one may try two sets of ξ_a and ξ_μ and compare the final results, if they coincide with each other, then the estimation is regarded as adequate. Otherwise, a new set of larger ξ_a and ξ_u may be tried. As a preliminary guide, we suggest

$$\xi_a=N_1\cdot RKS \quad , \quad \xi_u=N_2\cdot RKS \qquad RKS=Re(\omega/C_s) \quad , \quad N_2=N_1+100 \qquad (38)$$

N_1= 3 ~ 5 and N_2 = N_1 + 100. C_s is the S wave speed of the top layer. If some intermediate layer with low C_s exists, then a larger N_1 should be estimated. Integration of I_1 and I_2 may be carried out by four point Gaussian integration scheme. The integration of I_1 is performed down to the layer, where $\exp(a_m x_2)$ and $\exp(c_m x_2)$become insignificant and the interval of integration is recommended to be partitioned into $10N_1$ subintervals. According to our experience, assuming the upper limit $N_2=N_1+100$ is enough to get stable and accurate results, because radiation damping usually acts intensely.

NUMERICAL EXAMPLES

1. Dynamic compliance of visoelastic half-space

Load is distributed over an interval (-b/2, b/2) with unity resultant. Introducing dimensionless parameters

$a_0=\omega b/C_s$, $\beta=b\xi$

$\theta=2(1-\nu)/(1-2\nu)$, $\eta=(1+2i\zeta)^{-1}$

$\beta_1=(\beta^2-\eta a_0^2)^{1/2}$, $\beta_2=(\beta^2-\theta\eta a_0^2)^{1/2}$

$\beta_A=2\beta^2-\eta a_0^2$, $S_c=\sin(\beta/2)\cos(x_1\beta/2)$

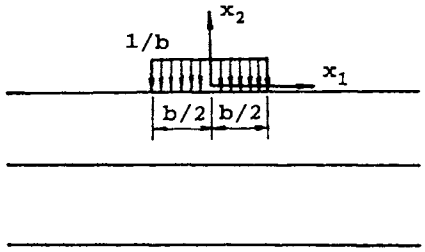

Halfspace

Fig.2 Dynamic Compliance of Layered Halfspace

Substitute (35) into (29) and (30) we get

$$u_{11}(x_1,0,a_0)=\frac{2a_0^2\eta^2}{\pi G}\int_0^{\infty}\frac{\beta_1 S_c}{\beta(4\beta^2\beta_1\beta_2-\beta_A)}d\beta$$

$$u_{22}(x_1,0,a_0)=\frac{2a_0^2\eta^2}{\pi G}\int_0^{\infty}\frac{\beta_2 S_c}{\beta(4\beta^2\beta_1\beta_2-\beta_A)}d\beta$$

$$u_{12}(x_1,0,a_0)=\frac{2\eta}{\pi G}\int_0^{\infty}\frac{(-2\beta_1\beta_2+\beta_A)S_c}{4\beta^2\beta_1\beta_2-\beta_A}d\beta$$

For a_0=0.5, ζ=0.25 and ν=1/3 , the results given by Dasgupta and Chopra (1979) are shown in Table II. The results calculated by the present procedure with N_2=100 (N_1=0) are shown in Table III. It took 4 sec. for calculation on a 386 computer. Results of Re(u_{11}) calculated with different N_2 are compared in table IV.

Table II Dynamic Compliance
(Dasgrpta and Chopra)

x_1/b	Re(u_{11})	Im(u_{11})	Re(u_{22})	Im(u_{22})
0.5	0.3548	-0.3902	0.2385	-0.3553
1.5	0.0707	-0.2899	0.0473	-0.2259
2.5	-0.0296	-0.2193	-0.1320	-0.1142
3.5	-0.0787	-0.1502	-0.1452	-0.0129
4.5	-0.0957	-0.0932	-0.1115	0.0620
5.5	-0.0929	-0.0501	-0.0531	0.1008
6.5	-0.0806	-0.0215	0.0085	0.1029
7.5	-0.0667	-0.0052	0.0566	0.0761

Table III Dynamic Compliance
(Present Procedure)

x_1/b	Re(u_{11})	Im(u_{11})	Re(u_{22})	Im(u_{22})
0.5	0.35475	-0.39022	0.23845	-0.35531
1.5	0.07061	-0.28985	0.04743	-0.22589
2.5	-0.03011	-0.21720	-0.13253	-0.11406
3.5	-0.07825	-0.15030	-0.14478	-0.01299
4.5	-0.09486	-0.09339	-0.11070	0.06181
5.5	-0.09241	-0.05020	-0.05268	0.10068
6.5	-0.08075	-0.02147	0.00837	0.10296
7.5	-0.06741	-0.00499	0.05583	0.07630

Table IV Dynamic Compliance of Re(u_{11})

x_1/b	N_2=10	N_2=50	N_2=100	N_2=200	N_2=1000
0.5	.35518	.35451	.35475	.35475	.35482
1.5	.07379	.07072	-.07061	-.07061	.07056
2.5	-.03195	-.03007	-.03011	-.03011	-.03012
3.5	-.08100	-.07823	-.07825	-.07825	-.07825
4.5	-.09544	-.09485	-.09486	-.09487	-.09487
5.5	-.09097	-.09240	-.09241	-.09241	-.09241
6.5	-.07957	-.08074	-.08075	-.08074	-.08075
7.5	-.06784	-.06740	-.06741	-.06741	-.06741

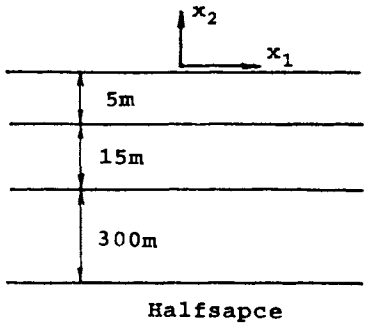

Fig.3 Multilayered System

2. Dynamic Compliance of a multilayered viscoelastic halfspace

Results for a multilayered system (Fig.3) with ζ=0.25 and $\mu_1:\mu_2:\mu_3:\mu_4$=1:2:4:5 are given in Table V. Results of an artificial layered system as shown in Fig.3 are given in Table VI, where each layer is assumed having the same elastic constants as in the preceding example and use N_1=3, N_2=103.

Table V Compliance of multilayered halfspace

x_1/b	Re(u_{11})	Im(u_{11})	Re(u_{22})	Im(u_{22})
0.5	0.42130	-0.38055	0.35926	-0.40417
1.5	0.10400	-0.33786	0.02075	-0.32895
2.5	-0.02854	-0.28293	-0.12462	-0.21894
3.5	-0.10804	-0.21687	-0.19444	-0.08886
4.5	-0.15015	-0.14777	-0.19984	0.03810
5.5	-0.16294	-0.08375	-0.15234	0.14013
6.5	-0.15432	-0.03118	-0.06957	0.20129
7.5	-0.13274	0.00637	0.02678	0.21428

Table VI Compliance of artificial layered system

x_1/b	Re(u_{11})	Im(u_{11})	Re(u_{22})	Im(u_{22})
0.5	0.35479	-0.39023	0.23850	-0.38533
1.5	0.07062	-0.28985	-0.04741	-0.22590
2.5	-0.03013	-0.21720	-0.13255	-0.11406
3.5	-0.07828	-0.15029	-0.14481	-0.01296
4.5	-0.09488	-0.09339	-0.11072	0.06181
5.5	-0.09240	-0.05020	-0.05268	0.10066
6.5	-0.08073	-0.02147	0.00838	0.10295
7.5	-0.06741	-0.00499	0.05583	0.07630

CONCLUSION

A new procedure for the evaluation of wavenumber integral of multilayered system is presented. The integral is split into two parts, corresponding to the range of plane waves and Rayleigh waves respectively. The former one is much narrower than the latter one. It has the advantages of achieving high degree of accuracy, while the computational effort is reduced to a great extent.

REFERENCES

Chen, H.H. (1993), "A Study of Gravity Dam-Reservoir Water-Soil Foundation Interaction Problems and its Application to Practical Engineering Projects", Doctoral Thesis, Dalian University of Technology, Dalian, China

Dasgupta G. and Chopra A. K. (1979), " Dynamic Stiffness Matrices for Viscoelastic Half Planes", ASCE 105, EM5: 729-745

Dunkin J. W. (1965), " Computation of Model Solutions in Layered Elastic Media at High Frequencies", BSSA, 55(2) : 335-358

Knopff L. (1964), " A Matrix Method for Elastic Wave Problems,", BSSA, 54(2) : 431-438

Xu P.C. and Mal A.K. (1987), "Calculation of the Inplane Green's Functions for a Layered Viscoelastic Solid", BSSA, 77(5) : 1823-1837